Int. J. Electrochem. Sci., 16 **(2021)** Article ID: 210219, doi: 10.20964/2021.02.50

International Journal of
ELECTROCHEMICAL
SCIENCE
www.electrochemsci.org

Hollow Gold Nanoshell Modified Electrode as Electrochemical Biosensor for Hemoglobin and Its Analytical Application

Xiaoqing Li[1,2], *Bo Shao*[1], *Yunxiu Sun*[1], *Bingxue Zhang*[1], *Xianghui Wang*[1,*], *Wei Sun*[1,*]

[1] Key Laboratory of Water Pollution Treatment and Resource Reuse of Hainan Province, Key Laboratory of Functional Materials and Photoelectrochemistry of Haikou, College of Chemistry and Chemical Engineering, Hainan Normal University, Haikou 571158, China;
[2] College of Health Sciences, Shandong University of Traditional Chinese Medicine, Jinan, 250355, China.
[*]E-mail: swyy26@hotmail.com and god820403@163.com

Received: 15 October 2020 / *Accepted:* 1 December 2020 / *Published:* 31 December 2020

In this paper hollow gold nanoshell (HGNs) was modified on carbon ionic liquid electrode (CILE), which was used for further immobilization of hemoglobin (Hb) with Nafion film step by step to get an electrochemical Hb sensor. UV-Vis absorption spectroscopy proved that Hb was not denatured after mixed with HGNs without change of the Soret band. Electrochemical studies proved the realization of direct electrochemistry of Hb on the HGNs/CILE and electrochemical parameters were calculated in details. Electrocatalysis, sample detection, and the stability of sensor were also investigated to show the analytical applications of this electrochemical sensor, which extended the usage of HGNs in electrochemical fields.

Keywords: Hollow gold nanoshell; Hemoglobin; Electrochemical sensor; Modified electrode; Carbon ionic liquid electrode

1. INTRODUCTION

Redox proteins (enzymes) can occur direct electron transfer process that similar to the electron transfer between molecules in organism to some extent. Therefore, electrochemical studies of redox proteins (enzymes) can understand the energy conversion and material metabolism of proteins, probe the structure and various physiochemical properties of biomolecules, and explore their physiological functions in life. The development of new types of biosensor has important theoretical and practical significance [1-4]. However, because the electroactive center of the redox protein is buried inside the protein, it is difficult to achieve direct electron transfer with ordinary used working electrodes [5].

Therefore, various modifiers are used to immobilize redox proteins to improve the rate of electron transfer [6-8].

As a kind of gold nanomaterial, hollow gold nanoshells (HGNs) show the advantages including high surface chemical energy, good stability, excellent biocompatibility, and large specific surface area. Aghadas et al. applied gold magnetic nanoshells modified gold electrode for electron transfer of homogenous hemoglobin (Hb) [9]. Okoth et al. used electrodeposition method to deposit gold nanoparticles (AuNPs) on the surface of ZnO-reduced graphene oxide nanocomposites. The good conductivity of AuNPs and the local surface plasmon resonance effect enhanced the photocurrent response and promoted electron transfer [10]. Ionic liquid (IL) is an excellent dielectric functional material in electrochemical researches [11, 12], which can be combined with traditional nanomaterials to form unique composites with synergistic effects [13-15]. Also IL can be acted as the electrolyte or the modifier in carbon paste electrode (CPE) [16]. Kong et al. investigated electrochemical behavior with ionic liquid 1-ethyl-3-methylimidazolium bromide as the binder in CPE [17]. In general IL modified CPE is denoted as carbon ionic liquid electrode (CILE), which shows high conductivity, good anti-pollution ability, excellent detection sensitivity and specific electrocatalytic activity [18, 19].

In this paper, HGNs and Hb were decorated on CILE to construct a third-generation electrochemical sensor (Nafion/Hb/HGNs/CILE). Because the original biological activity of Hb was retained, direct electrochemistry of Hb was achieved with electrochemical analysis to various substrates investigated carefully.

2. EXPERIMENTAL

2.1. Reagents

1-Hexylpyridinium hexafluorophosphate ($HPPF_6$>99%, Lanzhou Yulu Fine Chem. Co., China), bovine Hb (MW 64500, Sigma), Nafion polymer dispersions (5.0% ethanol solution, Beijing Honghaitian Tech. Co., China), HGNs (Nanjing XFNANO Materials Tech. Ltd. Co., China), graphite powder (average particle size 30.0 μm, Shanghai Colloid Chem. Co., China), trichloroacetic acid (TCA, Tianjin Kemiou Chem. Co., China), potassium bromate ($KBrO_3$, Shanghai Aladdin Biochem. Co., China) and sodium nitrite ($NaNO_2$, Shanghai Chem. Plant, China) were used directly. 0.1 mol/L phosphate buffer solutions (PBS) were prepared as the supporting electrolyte. Other chemicals were of analytical reagent grade with ultra-pure water used throughout.

2.2. Apparatus

A CHI 640E electrochemical workstation (Shanghai Chenhua Instrument, China) with traditional three-electrode system, including a Hb-modified working electrode, a platinum wire auxiliary electrode, and a saturated calomel reference electrode (SCE), was used. JEM-2010F transmission electron microscopy (TEM, JEOL, Japan) was used to record transmission electron

microscopic image. UV–Vis absorption spectrum was performed on a UV-5 spectrophotometer (Mettler-Toledo, Switzerland).

2.3. Preparation of Nafion/Hb/HGNs/CILE

CILE was home-manufactured by a procedure using $HPPF_6$ as the binder [20]. Then 8.0 μL of 0.5 mg/mL HGNs solution was casted on the CILE surface and dried naturally to get the HGNs/CILE, which was further coated by 8.0 μL of 15.0 mg/mL Hb solution and dried in the air. Finally, 6.0 μL of 0.5% Nafion solution was dropped on the electrode surface, and dried to obtain Nafion/Hb/HGNs/CILE. Other electrodes including Nafion/HGNs/CILE, Nafion/Hb/CILE, Nafion/CILE were also prepared similar to the above method.

3. RESULTS AND DISCUSSION

3.1. Characterizations

Fig.1A presented the TEM image of HGNs with different magnification sizes, which appeared like uniform spherical structure shell with the average diameters of 50 nm and uniform density distribution. The hollow three-dimensional structure can not only provide large specific surface area, but also can carry the protein.

UV-Vis absorption spectrum is applied to study the conformational change of protein and the Soret absorption band of Hb molecules can give data about the possible denaturation of the heme protein [21]. According to Fig.1B, the Soret absorption band of Hb aqueous solution (curve a) was located at 409.0 nm, same as that of Hb-HGNs mixed aqueous solution (curve b), indicating that Hb was not denatured and maintained its original conformation after contact with HGNs.

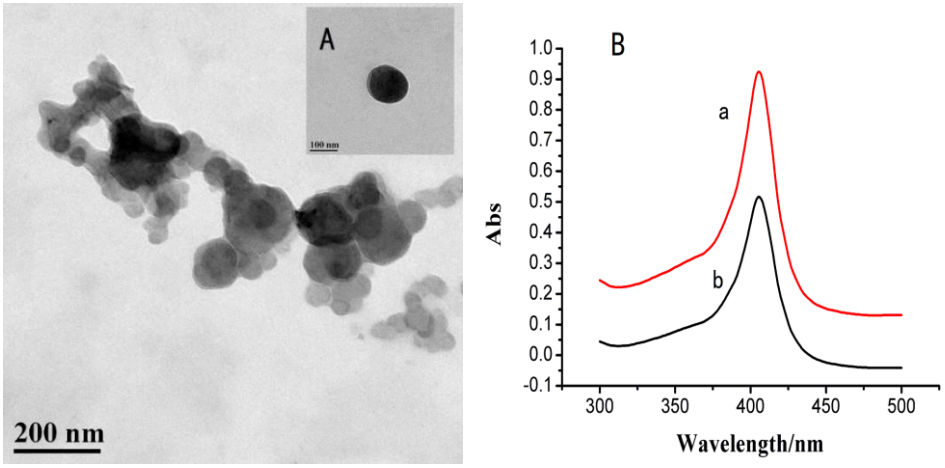

Figure 1. (A) TEM of HGNs at different magnification; (B) UV-Vis absorption spectra of Hb (a) in aqueous solution and (b) mixed with HGNs solution.

3.2. Direct electrochemistry

Electrochemistry of the different working electrodes was scanned by cyclic voltammetry in pH 3.0 PBS at the rate of 100 mV/s and the curves were shown in Fig. 2A. No responses occurred with bare CILE (curve a) and Nafion/CILE (curve b) in the potential range of investigation. On Nafion/Hb/CILE, a pair of redox peaks appeared (curve c), proving direct electron transfer of Hb with CILE happened due to the specific advantages of CILE. On Nafion/Hb/HGNs/CILE, a pair of redox peaks also appeared with enhanced peak currents (curve d), which was attributed to the modification of the HGNs on CILE. Gold nanomaterials are commonly used modifiers in electrochemical sensors with high metal conductivity, inherent catalytic activity, large surface area, and high loading capacity, which can form a conductive interface for Hb electron transfer with fast rate. From curve d the anodic (Epa) and cathodic (Epc) potential were located at −0.153V and −0.235 V (vs. SCE), respectively. The formal potential ($E^{0'}$) that calculated from the equation as $E^{0'}$=(Epa+Epc)/2, was got as −0.194V (vs. SCE), similar to the typical data of heme Fe^{III}/Fe^{II} redox couples [22]. The redox peak current had almost the same value. The results proved the characteristic electrochemical response of the Fe (III)/Fe (II) redox pair of the heme group.

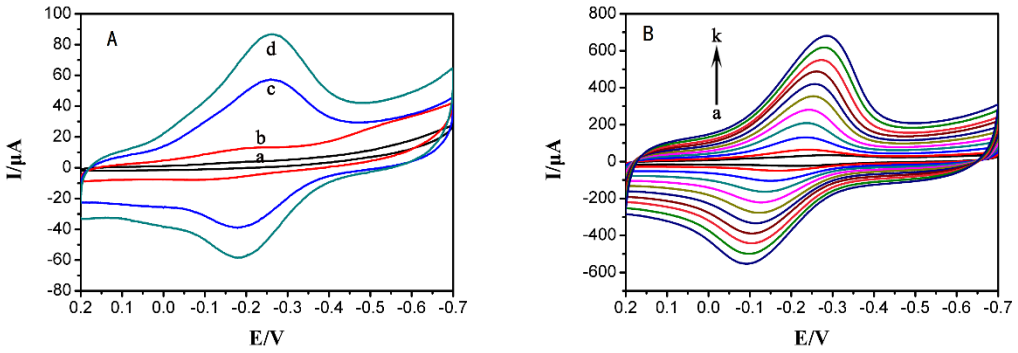

Figure 3. (A) Cyclic voltammograms of (a) CILE, (b) Nafion/CILE, (3) Nafion/Hb/CILE, (4) Nafion/Hb/HGNs/CILE in pH 3.0 PBS at a scan rate of 100 mV/s; (B) Cyclic voltammograms of Nafion/Hb/HGNs/CILE at different scan rates in pH 3.0 PBS (from a to k: 0.05, 0.1, 0.2, 0.3, 0.4, 0.5, 0.6, 0.7, 0.8, 0.9, 1.0 V/s).

Effects of scan rate on the redox responses of Hb were checked with cyclic voltammograms present in Fig. 3B. The currents increased linearly with rate from 0.05 to 1.0 V/s with the linear regression equations as Ipa (μA)= -69.483 υ (V/s)-1.183 (n=7, γ=0.998) and Ipc (μA)= 60.671 υ (V/s) + 6.264 (n=7, γ=0.997), proving a typical characteristic of surface-controlled thin-layer electrochemical behavior. The increase of scan rate led to the shift of the redox peak potentials with the enlargement of the peak-to-peak separation, demonstrating a quasi-reversible process. According to the Laviron's model [23, 24], the relationships of Ep versus *ln*υ were got with two linear regression equations as Epa (V) =0.039 lnυ (V/s) −0.108 (n= 8, γ =0.999) and Epc (V) =−0.060 lnυ (V/s) + 0.394 (n=8, γ=0.992). Then the values of the electron transfer coefficient (α), the apparent electron transfer rate constant (k_s) and the electron transfer number (n) were deduced as 0.397, 1.12 and 1.076 s^{-1}. The k_s value was bigger than that of Hb on other modified electrodes, such as Nafion/Co_3O_4-CNF/CILE

(0.92 s^{-1}) [25], Nafion/TNTs/CILE (0.85 s^{-1}) [26], BP-PEDOT:PSS/CILE (0.56 s^{-1}) [27], which indicated that the presence of HGNs was important for accelerating electron transfer.

3.3. Influence of buffer pH

The pH of buffer solution can affect the redox response of the heme proteins, and cyclic voltammetric behavior of Nafion/Hb/HGNs/CILE in different pH PBS was recorded with the curves shown in Fig. 3A. In the pH range from 3.0 to 8.0, a stable and well-defined redox peaks could be found with the peak potential ($E^{0'}$) gradually shifts to the negative potential with the increase of pH and the linear equation was $E^{0'}$(V) =-0.054 pH + 0.049 (γ = 0.999) (Fig. 3B). The biggest redox peak current at pH 3.0 PBS, which was selected as the supporting electrolyte. The slope value of -54.0 mV/pH is a little smaller than the theoretical value of -59.0 mV/pH at 25 ^{o}C for a one proton coupled one electron transfer process, which may be due to the different microenvironment of Hb molecules with same amounts of electrons in the electrochemical reaction [28].

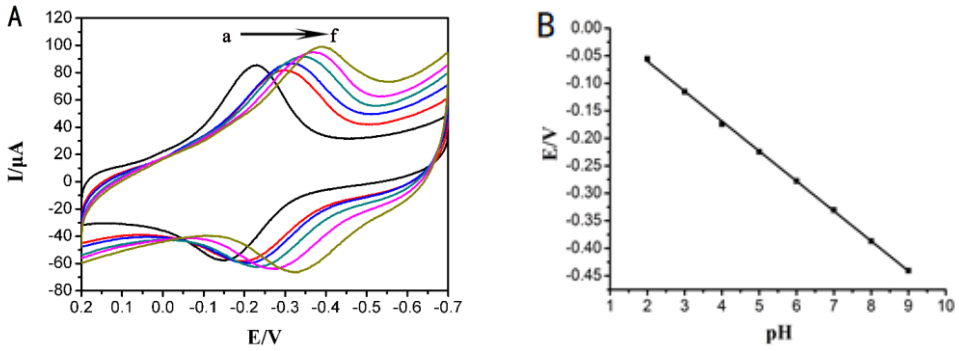

Figure 3. (A) Influence of pH on cyclic voltammograms of Nafion/Hb/HGNs/CILE with pH (a-f: 3.0, 4.0, 5.0, 6.0, 7.0, 8.0) at a scan rate of 100 mV/s; (B) The relationship between the formal potentials ($E^{0'}$) and pH.

3.4. Electrocatalytic activity

Due to the presence of Hb on the working electrode, electrocatalysis to various substrates was investigated in details. TCA is a disinfection by-product produced in the process of chlorination disinfection. Electrocatalysis of Nafion/Hb/HGNs/CILE to the TCA reduction were investigated with curves shown in Fig. 4A. An increase of the reduction peak current could be observed at -0.277 V (vs. SCE) and -0.514 (vs. SCE) after the addition of increasing concentrations of TCA in pH 3.0 PBS with the oxidation peak of Hb Fe (III) decreased gradually. A linear relationship was also obtained between the reduction peak current and the TCA concentration from 20.0 to 380.0 mmol/L (Fig.4B) with the regression equation as Ipa (μA) =748.43 C (mmol/L) +619.96 (n=10, γ=0.994), and the detection limit was estimated as 6.67 mmol/L. When the TCA concentration was larger than 380.0 mmol/L, the level off of the reduction peak current indicated a typical Michaelis-Menten kinetic process. The equation

$1/I_{ss} = (1/I_{max})\ (1 + K_M^{app}/C)$ was used to calculate the apparent Michaelis–Menten constant (K_M^{app}) with the result as 1.69 mmol/L, smaller as compared with some former references [29, 30].

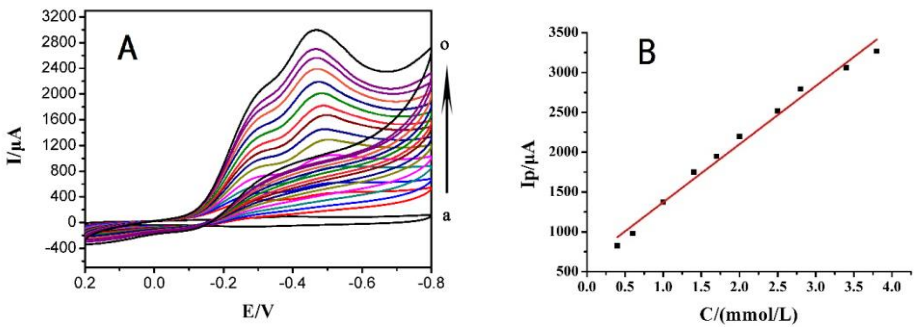

Figure 4. (A) Cyclic voltammograms of Nafion/Hb/HGNs/CILE in 0.1 mol/L pH 3.0 PBS with 0, 20, 30, 40, 60, 80, 100, 110, 140, 170, 200, 250, 280, 340, 380 mmol/L TCA (curve a-o) at the scan rate of 100 mV/s; (B) The relationship of reduction currents and the TCA concentration.

$KBrO_3$ is often used as analytical reagents, oxidants, wool bleaching agents and so on. Electrocatalytic effects to $KBrO_3$ were checked with cyclic voltammograms present in Fig.5A. A new reduction peak appeared at -0.261 V and the currents were linearly increased with $KBrO_3$ concentration from 0.1 to 9.5 mmol/L. The linear regression equation was Ipa (μA) = 14.05 C (mmol/L) + 65.15 (n = 10, γ = 0.990, Fig.5B) with the detection limit as 0.04 mmol/L (3σ). The Michaelis-Menten constant (K_M^{app}) was further deduced as 0.49 mmol/L.

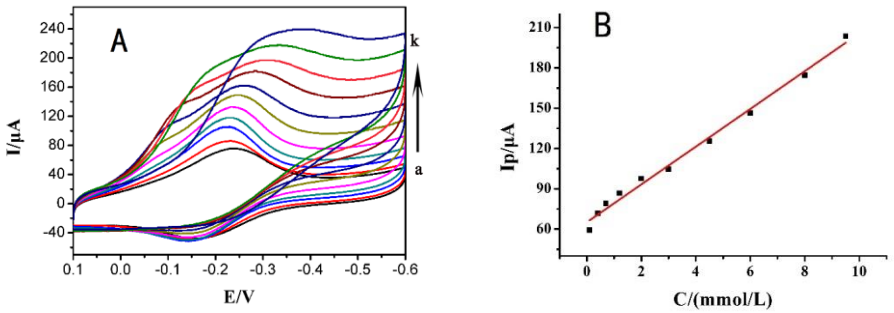

Figure 5. (A) Cyclic voltammograms of Nafion/Hb/HGNs/CILE in 0.1 mol/L pH 3.0 PBS with 0.0, 0.1, 0.4, 0.7, 1.2, 2.0, 3.0, 4.5, 6.0, 8.0, 9.5 mmol/L $KBrO_3$ (curve a-k) at the scan rate of 100 mV/s; (B) The relationships of reduction currents and the $KBrO_3$ concentration.

$NaNO_2$ is used in the processing of various meat products at home and abroad, which is harmful to human health and long-term consumption can cause cancer. Electrocatalysis of Nafion/Hb/HGNs/CILE to $NaNO_2$ was checked with curves shown in Fig.6A. The addition of $NaNO_2$ led to the decrease of the oxidation peak with the increase of the reduction peak at -0.716 V. A good linear relationship of $NaNO_2$ concentration with the currents was got from 0.1 to 25.0 mmol/L (Fig.6B) with the linear regression equation as Ipa (μA) = 3.54 C (mmol/L) + 53.47 (n=7, γ=0.991). The detection limit and K_M^{app} were calculated as 0.03 mmol/L (3σ) and 4.21 mmol/L. Table 1

compared the analytical performances of this method with different Hb modified electrodes, and the results showed that the method had a wide linear range and low detection limit.

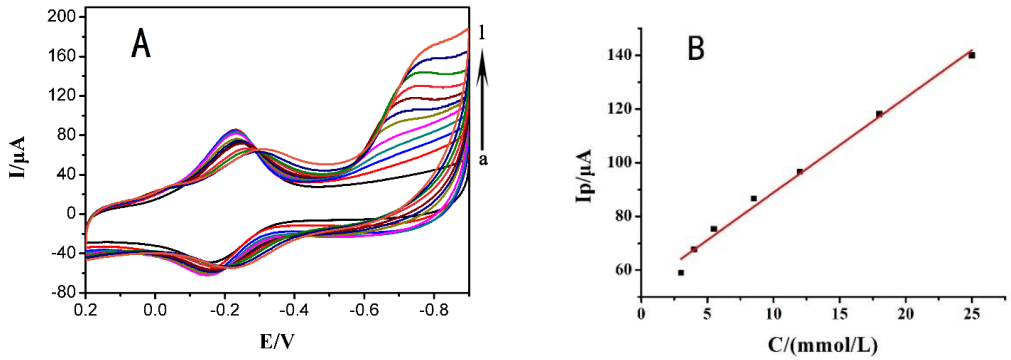

Figure 6. (A) Cyclic voltammograms of Nafion/Hb/HGNs/CILE in 0.1 mol/L pH 3.0 PBS with 0.0, 0.1, 0.5, 0.9, 1.6, 3.0, 4.0, 5.5, 8.5, 12.0, 18.0, 25.0 mmol/L $NaNO_2$ (curve a-l) at the scan rate of 100 mV/s; (B) The relationship of reduction currents and the $NaNO_2$ concentration.

Table 1. Comparison of analytical performances of different modified electrodes for nitrite analysis

Electrodes	Linear range (mmol/L)	LOD (mmol/L)	Refs.
Nafion/Hb/Co_3O_4-CNF[a]/CILE	1.0-12.0	0.33	25
Nafion/Hb/TNTs[b]/CILE	0.3-17	0.083	26
CTS/TiO_2-Hb/CILE	0.8-20	0.26	30
Nafion/Hb/Au/ZIF[c]-8/CILE	0.1-0.8	0.03	31
Nafion/Hb/GQD[d]/CILE	2-12	0.67	32
Nafion/Hb/HGNs/CILE	0.1-25.0	0.03	this work

[a]Carbon nanofiber (CNF), [b]titanate nanotubes (TNTs), [c]zinc-based metal organic framework material (ZIF), [d]Graphene quantum dots (GQD)

3.5. Stability of Nafion/Hb/HGNs/CILE

The long-term stability of the working electrode determines the sensing performance. Nafion/Hb/HGNs/CILE was put into the PBS and scanned continuously for 100 times under the condition of 100 mV/s by cyclic voltammetry, and no obvious changes were observed. After stored in a refrigerator at 4 ℃ for one week, the original peak response of Nafion/Hb/HGNs/CILE was still remained in 90% by 10 times cyclic scan at 100 mV/s, which demonstrated the good long-term stability of the electrode.

3.6. Samples detection

The fabricated electrode was used to determine real sample (Ika biological skin exchange solution) to investigate the practical application by calibration curve method. Also different concentrations of standard TCA aqueous solution were added to calculate the recovery by the standard addition method. The results were satisfactory with the recoveries from 94.66% to 108.25% (Table 2), showing the practical applications of this method.

Table 2. Analytical results of TCA samples (n=3)

Sample	Detected (mmol/L)	Added (mmol/L)	Total (mmol/L)	Recovery (%)
Medical facial peel	28.70	20.00	49.00	101.50
	32.70	40.00	76.00	108.25
	43.30	60.00	100.10	94.66

4. CONCLUSION

In this work, a novel electrochemical biosensor was prepared with HGNs and Hb modified CILE by layer-by-layer method with direct electrochemistry of Hb realized. The performances of the working electrode (Nafion/Hb/HGNs/CILE) was studied by cyclic voltammetry, which showed a pair of well-defined redox peaks. Electrocatalysis of Nafion/Hb/HGNs/CILE toward TCA, $KBrO_3$ and $NaNO_2$ was checked by cyclic voltammetry with satisfactory results. So the HGNs modified electrode is a potential electrochemical sensing platform for the third-generation biosensor.

ACKNOWLEDGEMENT
This work was financially supported by the National Natural Science Foundation of Hainan Province of China (219QN207), and Open Foundation of Key Laboratory of Water Pollution Treatment and Resource Reuse of Hainan Province (202003).

References

1. J. Rajbongshi, D.K. Das, S. Mazumdar, *Electrochim. Acta,* 55 (2010) 4174.
2. S.A. Bhakta, E. Evans, T.E. Benavidez, C.D. Garcia, *Anal. Chim. Acta*, 872 (2015) 7.
3. Y. Shao, Y. Jin, L. Wang, *Biosens. Bioelectron*., 20 (2005) 1373.
4. F.W. Scheller, N. Bistolas, S.Q. Liu, M. Janchem, M. Katterle, U. Wollenberger, *Adv. Colloid Interface Sci.*, 111 (2005) 116.
5. Y.Y. Niu, R.Y. Zou, H.A. Yones, X.B. Li, X.Y. Li, X.L. Niu, Y. Chen, P. Li, W. Sun, *J. Chin. Chem. Soc*., 65 (2018) 1127.
6. Q. Sheng, Y. Shen, Q. Wu, J. Zheng, *J. Solid State Electr.*, 20 (2016) 3315.
7. X.L. Wang, L.H. Liu, W. Zheng, W. Chen, G.J. Li, W. Sun, *Int. J. Electrochem. Sci*., 11 (2016) 1821.
8. S. A. Bhakta, E. Evans, T.E. Benavidez, C.D. Garcia, *Anal. Chim. Acta*, 872 (2015) 7.
9. B. Aghadas, G. Hedayatollah, *Clin. Biochem.*, 8 (2011) 532.
10. O.K. Okoth, K. Yan, J. Feng, J. Zhang, *Sensor. Actuat. B-Chem.*, 256 (2018) 334.
11. J.B. Zheng, Y. Zhang, P.P. Yang, *Talanta*, 73 (2007) 920.

12. D. Wei, A. Ivaska, *Anal. Chim. Acta*, 607 (2008) 126
13. Q. Zhao, D.P. Zhan, H.Y. Ma, *Front Biosci*, 10 (2005) 326.
14. C.Z. Lv, D. Chen, Z. Cao, F. Liu, X.M. Cao, J.L. He, W.Y. Zhao, *Int. J. Electrochem. Sci*., 11 (2016) 10107.
15. X.Y. Li, G.L.Luo, H. Xie, Y.Y. Niu, X.B. Li, R.Y. Zou, Y.R. Xi, Y. Xiong, W. Sun, G.J. Li, *Microchim. Acta*, 186 (2019) 304.
16. X.L. Niu, L.J. Yan, X.B. Li, A.H. Hu, C.J. Zheng, Y.L. Zhang, W. Sun, *Int. J. Electrochem. Sci*., 11 (2016) 1720.
17. L.D. Kong, Z.Y. Du, Z.Y. Xie, R.J. Chen, S.H. Jia, R.X. Dong, Z.L. Sun, W. Sun, *Int. J. Electrochem. Sci*., 12 (2017) 2297
18. X.F. Wang, Z. You, Y. Cheng, H.L. Sha, G.J. Li, H.H. Zhu, W. Sun, *J. Mol. Liq.*, 204 (2015) 112.
19. W. Sun, X.L. Wang, Y.X. Lu, S.X. Gong, X.W. Qi, B.X. Lei, Z.F. Sun, G.J. Li, *Mat. Sci. Eng. C-Mater*, 49 (2015) 34.
20. W.C. Wang, X.Q. Li, X.H. Yu, L.J. Yan, Z.F. Shi, X.Y. Wen, W. Sun, *J. Chin. Chem. Soc*., 63 (2016) 298
21. J.F. Rusling, A.E.F. Nassar, *J. Am. Chem. Soc*., 115 (1993) 11891.
22. Y. Xiao, H.X. Ju, H.Y. Chen, *Anal. Chim. Acta*, 391 (1999) 73.
23. X.J. Liu, T. Chen, L.F. Liu, G.X. Li, *Sens. Actuators B*, 113 (2006) 106.
24. Z. H. Chi, S.A. Asher, *Biochemistry*, 37 (1998) 2865.
25. H. Xie, G.L. Luo, Y.Y. Niu, W.J. Weng, Y.X. Zhao, Z.Q. Ling, C.X. Ruan, G.J. Li, W. Sun, *Mater. Sci. Eng. C-Mater.*, 107 (2020) 110209.
26. W.J. Weng, J.Liu, C.X. Yin, H. Xie, G.L. Luo, W. Sun, G.J. Li, *Int. J. Electrochem. Sci*., 14 (2019) 4309.
27. X.Y. Li, X.L. Niu, W.S. Zhao, W. Chen, C.X. Yin, Y.L. Men, G.J. Li, W. Sun, *Electrochem. Commun*., 86 (2018) 68.
28. R.A. Kamin, G.S. Wilson, *Anal. Chem*., 52 (1980) 1198.
29. T.R. Zhan, X.J. Wang, X.J. Li, Y. Song, W.G. Hou, *Sensor. Actuat. B-Chem*., 228 (2016) 101.
30. F. Shi, W.C. Wang, S.X. Gong, B.X. Lei, G.J. Li, X.M. Lin, Z.F. Sun, W. Sun, *J. Chin. Chem. Soc*., 62 (2015) 554.
31. J. Liu, W.J. Weng, C. X. Yin, G.L. Luo, H. Xie, Y.Y. Niu, X.Y. Li, G.J. Li, Y. Xi, Y.T.Gong, S.Y. Zhang, W. Sun, *Int. J. Electrochem. Sci*., 14 (2019) 1310.
32. X.Y. Li, H. Xie, G.L. Luo, Y.Y. Niu, X.B. Li, Y. R. Xi, Y. Xiong, Y.Chen, W. Sun, *Curr. Anal. Chem.,* 16 (2020) 308.